General Disclaimer

One or more of the Following Statements may affect this Document

- This document has been reproduced from the best copy furnished by the organizational source. It is being released in the interest of making available as much information as possible.

- This document may contain data, which exceeds the sheet parameters. It was furnished in this condition by the organizational source and is the best copy available.

- This document may contain tone-on-tone or color graphs, charts and/or pictures, which have been reproduced in black and white.

- This document is paginated as submitted by the original source.

- Portions of this document are not fully legible due to the historical nature of some of the material. However, it is the best reproduction available from the original submission.

STATION COORDINATES IN THE STANDARD EARTH III SYSTEM AND RADIATION-PRESSURE PERTURBATIONS FROM ISAGEX CAMERA DATA

E. M. Gaposchkin, J. Latimer, and G. Mendes

August 1975

Smithsonian Institution
Astrophysical Observatory
Cambridge, Massachusetts 02138

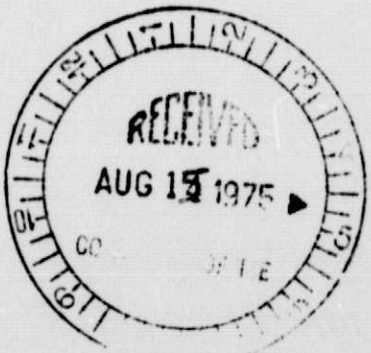

STATION COORDINATES IN THE STANDARD EARTH III SYSTEM AND RADIATION-PRESSURE PERTURBATIONS FROM ISAGEX CAMERA DATA

E. M. Gaposchkin, J. Latimer, and G. Mendes

ABSTRACT

Simultaneous and individual camera observations of Geos 1, Geos 2, Pageos, and Midas 4 obtained during the International Satellite Geodesy Experiment are utilized to determine station coordinates. The Smithsonian Astrophysical Observatory Standard Earth III system of coordinates is used to tie the geometrical network to a geocentric system and as a reference for calculating satellite orbits. A solution for coordinates combining geometrical and dynamical methods is obtained, and a comparison between the solutions and terrestrial data is made. The radiation-pressure and earth-albedo perturbations for Pageos are very large, and Pageos' orbits are used to evaluate the analytical treatment of these perturbations. Residual effects, which are probably of interest to aeronomists, remain in the Pageos orbits.

INTRODUCTION

The general objective of the International Satellite Geodesy Experiment (ISAGEX) was to "collect a set of homogeneous and well-distributed precise satellite observations for the purpose of dynamic and geometric geodesy considered as a first step towards the study of the earth as a complex

elastic body" (Brachet, 1970). ISAGEX was the natural successor to the 1967 Diademe campaign and the RCP 133 campaign in 1968-1969. A number of specific objectives were given in the ISAGEX experiment plan, which was divided into two phases: 1) the observation, reduction, collection, and distribution of data, and 2) investigations carried out by use of these data.

The actual observing campaign was also composed of two parts. The seven satellites then in orbit that were equipped with laser-tracking cube corners were routinely tracked by the satellite laser-tracking stations indicated in Figure 1. At the same time, a larger number of satellite-tracking cameras, also shown in Figure 1, observed these seven laser satellites plus two higher altitude satellites. Laser tracking was scheduled to obtain data for use in orbit computation and dynamical analyses, while camera tracking was planned to obtain simultaneous observations for geometrical analyses. The Geos 2 (6800201) flashing lights were used when possible. The observing program began in January 1971 and was completed at the end of that August. The catalog of data (Brachet, 1973) lists all reported observations.

By January 1972, the reduction of laser data had been completed. These data have been successfully used in global solutions for geopotential and station coordinates (see, e.g., Gaposchkin, 1973, 1974; Smith et al., 1973; Kovalevsky, 1974; Lerch et al., 1974). In these solutions, the ISAGEX data augmented existing satellite-tracking, terrestrial, and other data, and combined solutions were obtained. Data on as many as 26 satellites were used. The laser data were of sufficient quality and quantity to aid in establishing a global geocentric reference frame, which has an uncertainty of less than 5 m. In these solutions, camera stations providing both simultaneous and routine observations of sufficient quality and quantity are known with an uncertainty of less than 10 m.

The reduction of camera data from ISAGEX has now been completed; the data were distributed in June 1974, and the analysis of the observations has begun. Camera sites not determined in previous Smithsonian Astrophysical Observatory (SAO) solutions also contributed data, which have now been augmented by previously available data. The analysis of these new data is simplified in two ways. First, an existing geocentric network can be used as an established framework, with new sites referred to this system. Augmenting an existing network — that is, densification — is considerably simpler than establishing a fundamental network. Later, these data can be combined with existing ones in a general readjustment of the fundamental global network. Second, knowledge of both the earth's gravity field and the coordinates of fundamental stations, combined with the dense coverage of high-accuracy laser data, permits reference orbits to be computed for the satellites Geos 1 (6508901) and Geos 2 with an accuracy of better than 10 m.

GENERAL REMARKS

In addition to the basic geodetic objective of determining station positions, the analysis described here has two important aspects. First is the very powerful combination of the geometrical and dynamical methods using common data. Second is the critical nature of radiation-pressure effects when these periodic perturbations are large compared with the observation accuracy.

Although SAO has employed a combination of both geometrical and dynamical methods for 15 years, the base of observational data has been largely separate (except for Geos flash data) and little attempt has been made to cross check the data in a detailed manner. In the current analysis, such cross checking

has been very valuable. Data validation has been greatly speeded in many cases. More important, owing to the distribution of data, some stations are well determined by geometrical observations, and others, by dynamical observations. Therefore, by combining both, the strengths of both systems are exploited. In effect, both geometric and dynamic constraints on the analysis are important.

Radiation-pressure perturbations, direct solar and albedo, are the dominant perturbations for Pageos (6605601) because of its large area-to-mass ratio. The short-period perturbation is greater than 1 km. Computation of these perturbations depends on a number of physical quantities that are imperfectly known — e.g., the area-to-mass ratio, the exact geometrical shape, the points of exit and entry in shadow, and the earth's albedo. Complications with the physical model are compounded by analytical complexities. For example, it is currently unclear what form Kepler's third law takes, a law that relates the observed mean motion of the satellite to the semimajor axis of the orbit. Therefore, we cannot now fix the scale of an orbit dominated by radiation pressure merely from knowledge of the mean motion; these orbits cannot be used to establish the scale of a network. Therefore, the scale must be fixed by the three satellites with relatively small area-to-mass ratios: Geos 1 and 2 and Midas 4 (6102801).

The implications for a satellite like Lageos are obvious. This modified Kepler law must be known if Lageos is to provide scale by dynamical methods.

The analysis of the camera data presented a number of difficulties, which basically fall into two categories. First, the distribution of data in space and time was poor. Data on Geos 1 and Geos 2 were very sparse, so the extreme precision of the Geos orbits could not be completely utilized. A great many data were reduced for Pageos, but the resulting data were quite localized and had to be augmented with very low-precision radar data when used for orbit

computation. The number of simultaneous events finally used (184) is small, considering the 11,569 reductions performed. This first difficulty affects only the completeness of the result. The second difficulty concerns the necessity of validating the data critically; this task was complicated by a large uncertainty in the initial station coordinates and, for Pageos, in the radiation-pressure perturbations. The principal results of this process of simultaneously validating the data and improving the station coordinates can be summarized as follows. The quality of the AFU-75 data is reasonably good; that is, each sequence of 10 or more reductions is internally coherent to the expected 3 or 4 arcsec. However, large residuals result for many passes when the data are used in long arcs or in a geometrical solution for satellite position and station coordinates. Many of the residuals could be reduced to a reasonable level by applying a time correction.* This time correction corresponds to misidentification of the initial time mark on the film and is generally an integer second, corresponding to the interval between successive exposures.

Finally, the data validation and ultimate comparisons were more difficult because of the lack of geodetic information about many stations. Reliable datum coordinates, after suitable transformation, could provide geocentric coordinates of sufficient accuracy to validate and correct data. Also, geodetic coordinates provide a very useful check on the results. In the last analysis, only the sea-level heights were employed as a check, and they were not available for all the sites in question.

---

*Karsky et al. (1974) note that all nonflash observations for station 1147 (Ondrejov) have random timing uncertainties. No attempt was made to treat these data in a special way.

ORBIT ANALYSIS

To analyze tracking data by dynamical methods, the greatest orbit accuracy is necessary. Each aspect of orbit computation presents a number of problems. Among these are knowledge of the earth's gravity field, the earth's body and ocean tides, the position of tracking stations, understanding and solutions of the equations of motion under the influence of gravitational drag and radiation pressure, observations and reduction of observations in a uniform coordinate and time system, and estimates of the constants of motion and other physical parameters by use of models and observations.

For the purpose of this discussion, we present an estimate of ephemeris accuracy. Geos 1 and 2 are well observed with 1-m accuracy from a global distribution of laser stations. Other components in the error budget for these orbits are much larger, the largest error source being the limited knowledge of the earth's gravity field. Therefore, the accuracy of these orbits is estimated from the orbital fit to the data for arcs of 10 days and longer. Midas 4 is higher in altitude, and uncertainties due to the earth's gravity field are therefore reduced. However, the only data with an accuracy of 4 arcsec available from a global network of stations are camera data. Since the orbital accuracy is expected to be more precise than the accuracy of an individual observation, no direct estimate of accuracy is available. The higher orbital accuracy relative to observational accuracy is confirmed by the standard error of unit weight of the orbital fit being less than 1. The orbital accuracy is therefore estimated from the internal consistency of the observational residuals, the consistency of the mean orbital elements, and the scaling of gravity-field model errors as a function of height. Pageos is

in a far less favorable situation than is Midas 4, but both have very similar orbital characteristics (i.e., high inclination, modest eccentricity, and high altitude). However, during the interval under consideration, 4-arcsec data are available primarily from cameras in a limited geographic area in Europe, Eurasia, and North Africa (see Figure 2), which results in very limited orbital coverage: less than 20° in the satellite's true anomaly at best. In addition, the effects of photon pressure from direct solar radiation and earth's albedo radiation are significant and become the most important perturbations. Therefore, the uncertainty in calculating nongravitational perturbations due to unknown physical properties and to theoretical detail not yet fully developed imposes the limiting accuracy in orbit computation.

In all orbits used in this analysis, the gravity field and station coordinates were taken from the 1973 Smithsonian Standard Earth (III) (SE III) (Gaposchkin, 1973), with the additional constants given in Table 1. Long- and short-period gravity-field perturbations, lunar and solar perturbations including solid body and ocean tides, and radiation-pressure and albedo-pressure perturbations were applied in all computations. The effect of drag was modeled with an empirical acceleration in the mean anomaly, as has been done for years.

ORBITAL ACCURACIES

Geos 1 and Geos 2

The present accuracy of orbit computation for Geos 1 and Geos 2 is better than 10 m. Based largely on laser data obtained during the ISAGEX, this accuracy was documented in SE III (Gaposchkin, 1973) and is confirmed here and in subsequent analyses. Briefly, this accuracy has been estimated from three calculations:

A. Analysis of laser residuals in the orbit determination.

B. Consistency of the mean elements for independently determined contiguous orbits.

C. A systems simulation that employs error models for the total system (gravity field, orbit theory, observations, station coordinates, and other parameters).

Orbital coverage with these data was not complete; however, the residuals are consistent with an orbital accuracy better than 10 m. The residuals may be optimistic, in that they are departures for a specific model that uses orbital parameters determined so as to minimize these residuals. Residuals reveal neither systematic errors in observed positions nor errors in the unobserved segments of the orbit. The orbital elements can provide a measure of these effects. If the orbital theory were without error, then the orbital parameters a, e, and I should be constant for all time and should have secular changes. Examination of the mean elements evidences long-period variations in them, and they are being studied. The internal coherence of the mean elements is consistent with a 10-m accuracy.

SAO has developed a total system computer simulation for evaluating the laser system. Included in the simulation are a gravity-field error model derived from SE III, 1.5-m errors in station positions, random and systematic errors in the laser data themselves, and error models for other geophysical parameters such as GM, k_2, refraction, polar motion, and UT1. The orbital residuals and internal consistency of the orbital elements are in almost complete agreement with those obtained from treating the actual data. Although the orbital elements constitute the weakest link in achieving sub-10-m accuracy, they remain consistent with the error budget.

Midas 4

Four-arcsec camera data have been obtained from a global network for Midas 4. With a height of 3500 km, this satellite is less affected by errors in the geopotential than Geos 1 or 2. Thus, longer arcs can be computed. From the available data, we selected two arcs, 33 and 48 days in length. The standard errors of unit weight are 0.84 and 1.15, respectively, indicating that the model has fitted the data as well as can be expected in a statistical sense. Therefore, we conclude that the orbital errors are less than the observation errors.

Pageos

Orbit computation and its accuracy estimate for Pageos are complicated by four factors not present for the above three satellites:

A. A limited set of observations.

B. The uncertainty of photon-pressure perturbations.

C. A possible unmodeled resonance with the earth's gravity field.

D. The uncertainty in station coordinates.

All observations of Pageos were made from camera stations shown in the network schematic in Figure 2, resulting in very local orbital distribution (less than 20° in true anomaly). Furthermore, the data are spread unevenly throughout the time of ISAGEX: Many orbits contain data from no more than three stations.

For Pageos, the perturbations due to direct solar radiation and albedo reradiation pressure are three orders of magnitude larger than for Geos 1, Geos 2, and Midas 4. The short-period perturbation from direct solar radiation pressure is of the order of 1 km and constitutes the dominant effect in Pageos orbits. The computation of these perturbations is critical for obtaining accurate Pageos orbits.

Semianalytical developments for determining these perturbations (Aksnes, 1975; Lautman, 1975a,b) assume the following:

A. The satellite is spherical with constant reflective properties.

B. The solar parallax can be neglected.

C. The solar flux is constant.

D. The earth's albedo varies from pole to equator as a function of $a_0 + a_2 \sin^2 \phi$.

E. The infrared radiation varies from pole to equator as a function of $b_0 + b_2 \sin^2 \phi$.

None of these assumptions is strictly true, and surely A causes predictable effects in the analysis described here.

Three critical aspects of the radiation-pressure treatment have been studied. First, the interaction between gravitational perturbations and radiation-pressure perturbations were carefully computed. Since these perturbations plus gravitational secular perturbations, gravitational long-period perturbations, and radiation-pressure long-period perturbations are all of order 10^{-3}, their interactions become larger than 10^{-6}. The interaction between the secular gravitational perturbation and the radiation-pressure perturbations has been encorporated. Second, the integrated perturbations were computed along the lines of Kozai (1961, 1963); they depend on the value of the eccentric anomaly of the satellite both at shadow exit and entry when shadowing occurs and from perigee passage to perigee passage when shadowing does not occur. The formulas by Kozai (1961, 1963) and used by Aksnes (1975) were derived assuming that λ (the longitude of the sun), ω, Ω, i, e, and a are constant in one revolution. This is, of course, not strictly true, and in principle, a second-order solution to the Kozai equations would have to be developed for this effect to be incorporated. However, by including the changes

in λ, ω, and Ω in one revolution in the computation of shadow exit and entry with shadowing and in the time from perigee passage to perigee passage without shadowing, the bulk of the effect is satisfactorily computed. Aksnes (1975) provides a numerical comparison between the analytical theory and a numerical integration. With this generalization, the theory seems to be of sufficient accuracy to treat the Pageos data. A shadow model is defined by incorporating the oblateness of the shadow due to the earth's oblateness, and a numerical computation of the shadow point is made by iteration to within 100 m. The critical nature of shadow exit and entry opens the question of penumbral effects and refraction effects. Although there is no evidence from the orbital residuals that our model needs improvement, the question deserves further study. Finally, it has become apparent that the relation between the observed mean motion, with short-periodic perturbations removed, and the mean semimajor axis is unclear. The problem is solvable; the analysis of Pageos data proceeded by solving for this relation from the observations — that is, we used the mean motion and the semimajor axis as independently determined orbital parameters. The effect for Pageos may be as large as 1000 m, which has implications for future satellites such as Lageos. The effect for Lageos can be directly scaled by the ratio of the area-to-mass ratios.

To analyze Pageos data with an accuracy comparable to 10 m requires knowledge of its area-to-mass ratio A/m to 1% and of the earth's albedo α to 10%. Mean elements determined from orbits computed with camera and radar data were used to estimate the optimum A/m. These orbits covered an interval of 120 days. Figure 3 gives "observed" mean elements for this period after radiation-pressure perturbations were removed. The A/m was chosen by using the eccentricity and inclination. Perturbations due to drag were computed by Slowey based on

techniques previously described (Slowey, 1974). From other analyses (Smith and Kissel, 1971; Prior, 1970; Lucas and Chovitz, 1971), there is evidence that Pageos has a slight oblateness, which gives rise to large long-period perturbations in the semimajor axis when shadowing occurs. Figure 4a plots the acceleration of Pageos, which does not seem to show up in the data analyzed. However, in Figure 4b, the 10.7-cm solar-flux index clearly indicates that some atmospheric or magnetospheric effect is present. A value of

$$A/m = 132 \pm 4 \text{ cgs}$$

is obtained, which compares favorably with the prelaunch specifications for Pageos:

$$A/m = 136 \text{ cgs}.$$

The satellite thus appears to be a specular reflector with about 3.4% absorption. This value is used for computing radiation-pressure and albedo-pressure perturbations. The orbital residuals are consistent with both a 4-arcsec observation accuracy and the standard error of unit weight obtained for the orbits.

Pageos has a strong resonance with terms of 8th order in the earth's gravity field. At the time of the ISAGEX program, the principal resonant period was approximately 40 days. Thus, 8-day arcs were computed to absorb the possible unmodeled resonant effects in the mean orbital elements and to eliminate that corrupting effect on the ephemeris computation.

The large uncertainty in station coordinates, the relatively small number of stations contributing to our orbit, and the possible errors in the data made computation of orbits quite uncertain. Although the coordinate accuracy and validation of the data were eventually resolved, the relatively poor distribution in each orbital arc remains a source of concern.

In summary, the reference orbits are known for Geos 1 and Geos 2 to better than 10 m; for Midas 4, between 10 and 20 m; and for Pageos, probably no better than 50 m. In all cases, this accuracy is sufficient to analyze camera data with an accuracy of 40 m for Geos 1 and Geos 2 and 100 m for Midas 4 and Pageos, in good agreement with the standard error of unit weight for each orbital arc. The Geos 1 and Geos 2 orbits contain laser data, and the standard error reflects the orbital error. The laser data are assigned an uncertainty of 5 m. The Midas 4 orbital residuals are due to random observation errors. The Pageos orbits with sufficient data have observation errors and errors in radiation-pressure modeling. Several Pageos orbits have $\sigma_0 < 0.5$, indicating that the ephemeris accuracy is indeed better than the observation accuracy.

VALIDATION OF CAMERA DATA

Camera data taken during ISAGEX have been used both for determining station coordinates and for analyzing satellite orbits. By use of simultaneous observations in a geometrical analysis and of routine observations in orbit computation, the locations of stations have been determined. These two methods have also been used in combination. A dynamical determination of site locations depends on a precision orbit computation, as discussed earlier. Preliminary analysis of the ISAGEX camera data (Gaposchkin et al., 1974) has been encouraging; the camera data are good, and the resulting coordinates have proved realistic.

A significant number of camera data were discarded in both the geometrical adjustment and the orbit computation. The observed residuals were so large that they could not be attributed to random observation errors. Furthermore, the residuals were almost always coherent; that is, a sequence of 10 positions would have nearly the same residuals in both right ascension and declination.

Using an ephemeris that was believed to be accurate as a reference, we examined the residuals for possible evidence of station timing. Integer-second corrections to the observation times produced residuals in right ascension and declination that were realistically attributable to the expected random observation error. This was true for data from all four satellites used in this investigation. Such corrections could be attributed to a possible misidentification of the beginning of a satellite pass at the station. Such data recovery was critical for both the dynamical and the geometrical solutions. For example, in the geometrical solution, before comprehensive data editing and retrieval, 112 good satellite positions were obtained. Finally, 182 good satellite positions were used.

The overall computation was set up in a large-scale iteration. With a finite amount of data, ambiguity can arise between corrections to station timing and corrections to station coordinates plus corrections to the satellite ephemeris. The iterative process established is outlined in Figure 5, with the following guidelines. First, we categorized the orbits into two classes:

A. Orbits with sufficient data from well-known stations with a priori orbit accuracy (i.e., Geos 1, Geos 2, and Midas 4).

B. Orbits that needed close study because of initially uncertain perturbations due to radiation pressure or gravity-field resonance and because of restricted distribution of tracking data (i.e., Pageos).

Second, the stations were separated into three groups:

A. Stations whose coordinates were initially known with sufficient accuracy for orbit computation; these stations had enough simultaneous data and routine data from several orbits that did not need corrections and could be used to obtain both orbit ephemerides and improved coordinates. These Group I stations were

Uzhgorod, USSR	1055
Riga, Latvia	1084
Cairo, UAR	1901
Potsdam, DDR	1181
Delft, Netherlands	8034
Zvenigorod, USSR	1072

B. Stations with data in several orbits, some of which did not require time corrections and for which some simultaneous events would be available as a check. The stations comprising Group II were as follows:

Ondrejov, Czechoslovakia	1147
Baja, Hungary	1113
Bucharest, Romania	1131

C. Stations not falling into A or B. Except for Sofia (1101), these stations were observed in few orbits and had no simultaneous observations.

Group III stations included:

Sofia, Bulgaria	1101
Sakhalin, USSR	1065
Ulan Bator, Outer Mongolia	1660
Kerguelen Island	1108

Next, corrections to station timing were generally computed only for a sequence of 10 or a multiple of 10 observations that had coherent residuals. Also, no attempt was made to determine time corrections for Ondrejov (1147), as all Geos 2 passive observations had random timing errors (Karsky et al., 1974).

Finally, the initial coordinates were estimated, at worst, to be in error by several kilometers, except for Sakhalin, Ulan Bator, and Kerguelen Island. Since the satellite velocity is approximately 8 km sec^{-1} and the ephemeris

accuracy is certainly better than 1 km, apparent timing errors greater than 1 sec were assumed to be timing and not orbital or station-coordinate problems. The number of observations that fitted very well after integer-second corrections were made, even with approximate station coordinates, gave confidence in this method of analysis.

Starting with the stations in Group I, improved coordinates and timing corrections were determined. As the orbits improved (especially for Pageos), station timing corrections for Groups II and III were obtained. If revised timing corrections were available, the iterative procedure returned to level A in Figure 5. Otherwise, the iteration proceeded from B. Furthermore, special attention was paid to corrected simultaneous observations to verify that indeed the time correction improved both the fit with the simultaneous direction and the orbit computation. It is important to note that not all errors can be removed by a timing correction; the time adjusts only the along-track component, corresponding to the declination. A more detailed discussion of each phase of the computation indicated in Figure 5 is given in subsequent sections of this report.

Table 2 gives a breakdown by station and satellite of the data available for analysis. The camera data used in the preliminary analysis (Gaposchkin et al., 1974) are listed in Table 3, and the total number of camera observations utilized in the analysis by satellite arc and stations is presented in Table 4.

THE GEOMETRICAL ANALYSIS

Data

The first step in the geometrical analysis was to sort the data chronologically by satellite in order to extract simultaneous observations. The data were then processed according to the method described in Aardoom et al. (1967)

to derive synthetic simultaneous observations. A very few individual observations were eliminated because the polynomial-fitting procedure for the nonflash data revealed some grossly bad data points. At this stage, there were 317 satellite positions, consisting of 683 synthetic observations and 2346 actual observations (see Table 5). Only 20% of the 11,569 precisely reduced observations were potentially useful for a geometrical analysis.

With these data, we began preliminary network adjustments using the techniques of SE III. Data were deleted from the final adjustments for any of the following reasons:

A. The data involved only well-determined SE III stations with little likelihood of improving interstation directions (e.g., 9004-9030).

B. The data were insufficient to permit a good determination by the geometrical method (e.g., 1101 and 1660).

C. Network-adjustment residuals were too large.

D. Orbital-determination residuals were too large.

By comparing residuals from the orbital method with those from the geometrical method, it was possible in a few instances to delete single bad observations and to improve the interpolated synthetic observations. The simultaneous data utilized in the final adjustments are summarized in Table 6. Evidently, about 50% of the potential simultaneous data are actually useful. This corresponds to about 12% of the total precisely reduced optical data set.

The Adjustment

In describing a network adjustment, it is useful to look at the synchronous planes involved. Each such plane contains two stations and one satellite position. Six stations whose coordinates in the SE III system are reasonably well determined were not adjusted. Listed in Table 7, these stations were called fixed stations. A satellite simultaneously observed by n stations will give p synchronous planes for further adjustment, where

$$p = \begin{cases} \sum_{j=1}^{n-1} j - \sum_{j=1}^{k-1} & k \geq 2 \\ \sum_{j=1}^{n-1} j & k < 2 \end{cases},$$

and k is the number of known stations in the simultaneous event.* Therefore, one measure of the strength of our network is indicated by tabulating the number of adjustable synchronous planes between each pair of stations (see Table 8) and by mapping the network (see Figure 6).

To strengthen the network, information was added in the form of eight interstation directions from previous observation campaigns. Six of these were the same as those previously used in the SE III geometrical adjustment; two additional interstation directions were taken from Georgiev and Sorokin (1975). They were treated as observations, not constraints, and were weighted proportionally to the inverse of their covariances. They are mapped in Figure 6. The original

*The second summation is dropped if $k < 2$.

six directions are actually composed of 218 synchronous planes and 436 synthetic (or flash) observations. They have been included in two adjustments (SE III and here), and in both instances, the residuals are a bit higher than would be expected from their a priori covariance matrices. (The root mean square of the residuals is twice the a priori sigma.)

The weighting matrices of the pre-ISAGEX interstation-direction data were scaled down by a factor of 2, a factor we believe to be reasonable. It does not greatly affect the adjustment, but it does shift weight to the newer ISAGEX data. Flash observations (constituting over 60% of the synthetic observations in the final ISAGEX data set) were assigned a uniform variance of 4 arcsec^2 in each dimension. The variance was computed for passive synthetic observations from the polynomial-fitting procedure but was assigned an arbitrary lower bound of 1 arcsec^2 in each dimension. The correlation in a coordinate system oriented along and across the satellite's apparent motion was arbitrarily set to zero. Variances along track tend to be higher than those across track. All synthetic observations must be better than 10 arcsec to be used in our adjustment. Typical variances would be from 2 to 4 arcsec^2 along track (after lower bounding) and 2 to 3 arcsec^2 across track for ISAGEX data.

There are two adjustments. Potsdam (1181) observed simultaneously only with Malvern (8011) and San Fernando (9004) (a fixed station) and hence was entirely uncorrelated with the rest of the network. The adjustment for Potsdam gave a standard deviation of 0.79. This is probably optimistic, because only 30 synthetic observations were included. The adjustment for the remainder of the network (including the pre-ISAGEX interstation-direction data) gave a standard deviation of 1.36. This is reasonable, undoubtedly reflecting the existence of some unaccounted-for systematic errors. Each of the two geometric components of the combination solution was weighted in accordance with the variances of unit weight.

DYNAMICAL SOLUTION

The computation of station positions according to the orbital method is described in Gaposchkin et al. (1974) and depends on the computation of a precision ephemeris. The orbital arcs selected for this analysis are listed in Table 9, and the accuracy of both the orbit and the ephemeris calculation was given above.

The scale of the geodetic network is imposed by the scale of the satellite orbit, which is obtained through Kepler's third law:

$$GM = n_0^2 a_0^2 \quad . \tag{1}$$

By definition, this relation holds for the oscillating mean motion n_0 and the oscillating a_0. Therefore, $n_0 = dM/dt$. In practice, we can compute the mean elements $\bar{n}$ and $\bar{a}$, and equation (1) becomes

$$GM = \bar{n}^2 (1 + f)^2 \bar{a}^3 (1 + g)^3 \quad , \tag{2}$$

where f and g are functions defined by the particular perturbation theory employed. The most familiar form of equation (2) accounts for the secular change in the mean motion, due to the zonal harmonics, to first order:

$$a = \left(\frac{GM}{n^2}\right) \frac{1}{3}\left[1 + \frac{1}{3}\frac{J_2}{p^2}\sqrt{1 - e^2}\left(-1 + \frac{3}{2}\sin^2 I\right)\right] \quad ,$$

$$P = \left(\frac{GM}{n^2}\right)^{1/3} (1 - e^2) \quad . \tag{3}$$

Higher order expressions are given by Brouwer (1959), Kozai (1962), and Aksnes (1969). The advantage of this approach is that the mean motion $\bar{n}$ (free from short-period perturbations) can be determined very accurately from observations. With perturbations derivable from a potential, there are no long-period perturbations in a, and therefore equation (2) can be used to define

the size of the orbit and hence the scale of the geodetic network. For Geos 1 and 2 and Midas 4, the short-period perturbation due to radiation pressure is small enough that an error in scale introduced by the uncertainty of its mean value can be ignored. For Pageos, this is not true. In this analysis, the scale of the orbit and the mean motion are determined separately for each Pageos arc. This can be viewed either as a change in GM or as an empirical computation of $\delta\alpha_o$ due to radiation pressure. In either case, the satellite scale is obtained by transferring the terrestrial scale, as specified by the coordinates, to the satellite via the observations. Consequently, Pageos orbits do not contain any information on scale, as the correction δGM is eliminated by the method of reduced normals in the combination of satellite orbits. The scale of the geodetic net is therefore established by observations of Geos 1, Geos 2, and Midas 4. Unfortunately, there are far fewer observations of these satellites from the stations in question. However, the orbits for Geos 1 and 2 are based on a global distribution of laser stations, and the metric scale for these satellites is excellent.

Each orbital arc was computed by use of 10 to 14 unknown parameters. In general, linear functions were determined for the perigee, node, and eccentricity; a constant was used for the inclination, and a quartic or quintic polynomial was utilized for the mean anomaly.

The first three iterations were solved for the six Group I stations. Individual orbit solutions were made for Group III, and when deemed satisfactory, these stations were added to the set of unknowns in a global solution. Each orbital arc was computed with the full set of normal equations for the orbital elements, supplementary parameters, and station coordinates. All orbit-dependent parameters were eliminated by the method of reduced normal equations, thereby completely

preserving the covariances of all unknowns. The last comprehensive solution contained all the stations given in the final results except for Sofia (1101), Baja (1113), and Bucharest (1131).

COMBINATION SOLUTION

The normal equations for the geometrical solution and those for the dynamical solution for coordinates (with all other parameters eliminated by the method of reduced normal equations) were combined, and a joint solution was obtained.

Possible systematic differences in orientation between the reference frames used for the individual analyses were investigated. Such differences, which were found in global solutions for coordinates (see, e.g., Gaposchkin, 1973), can arise only from implementation of computer programs. The geometrical analysis is done in a terrestrial system, whereas the dynamical analysis is performed in a quasi-inertial reference frame. However, for determining station coordinates, both computations are designed to refer corrections to the same reference system. The cause of specific differences in global solutions remains unknown. For this network adjustment, systematic rotation parameters between the two systems were introduced in the normal equations. There can be no difference in origin or scale, since both analyses used the same fixed stations. The rotation parameters were found to be insignificant, indicating that the number of data and the network geometry did not allow a meaningful discussion of differences in orientation. Therefore, the adopted solution was made by assuming that the two systems are identical; the adopted solution is given in Table 10.

The parameters determined are the geocentric rectangular station coordinates. Direct comparisons of the geocentric, geometric, and dynamic coordinates are not really meaningful, as the coordinates for each station are not all determined with equal accuracy. Comparisons of the observed directions, the dynamical solution, and the combination solution are given in Figure 7.

The geodetic coordinates of the determined sites are generally not available. However, for many of the sites, an estimate of the mean sea level (h_{msl}) is available. Using this estimate together with the geoid height, the height above the ellipsoid can be computed; this, in turn, can be compared with the ellipsoid height determined from the coordinates. The geoid height and ellipsoid can be taken from global analysis or from the datum. For this comparison, we give both values in Table 11. The global values of geoid height and ellipsoid are taken from Gaposchkin (1973). The Europe 50 (EU 50) datum coordinates are determined from the datum shifts given in Gaposchkin (1973). Both comparisons indicate a 10- to 20-m accuracy. In both cases, the height comparison for Delft and Zvenigorod is quite large. There were only 47 points from Delft, and all were from one satellite (Geos 2). Even so, the agreement is not so good as could be expected in comparison with other stations. The comparison for Zvenigorod is similarly large and negative. In this case, the mean-sea-level height may be in error, as its value could not be checked. Also, Zvenigorod is at the edge of the geometrical network, which could lead to amplification of even small systematic errors in the data. Furthermore, in determining the datum shift, rotation, and scale for the Europe 50 system, Gaposchkin (1973) did not have a station in the neighborhood. Therefore, use of these datum-transformation parameters must be viewed as an extrapolation, which could introduce errors. Any or all of these factors could come into

this comparison. There remains the question of the large (10-m) systematic negative values for the global geoid comparison, especially in Europe. These values could be due to the limited number of observations on Geos 1, Geos 2, and Midas 4, which determine scale in the dynamical analysis. However, scale is imposed on the geometrical solution by the fixed stations. This could be a regional feature. The satellite geoid or the mean-sea-level heights may have some systematic regional bias. Extensive tests of satellite geoids indicate that they are expected to be no worse than a 3-m uncertainty in regions where surface gravimetry exists: the case for Europe. The mean-sea-level heights can easily be determined to better than a meter if sufficient data are taken and analyzed properly. This could also be related to the systematic 1-ppm scale difference found between dynamical and geometrical analyses. Therefore, one of the above assertions must be wrong. Resolution of this question must await further improvements in satellite-determined station coordinates, gravity fields, and mean-sea-level heights.

In conclusion, the coordinates are determined to be between 15 and 20 m, as indicated by the formal uncertainty, the comparison of interstation directions, and the comparison of the heights. Such a result is quite consistent with SAO's 1966 determination (Lundquist and Veis, 1966), where 10 to 20 m was quoted for stations with approximately 50 simultaneous observations and sufficient individual observations.

SUMMARY

A. The camera data obtained during the ISAGEX program have been used to determine station coordinates with an accuracy of 10 to 20 m by combining geometric and dynamic analyses.

B. The short-period perturbations due to radiation pressure must be taken into account to compute satisfactory orbits for the Pageos satellite.

C. During the period studied (1971), no evidence of anomalous acceleration due to satellite oblateness was found.

D. The area-to-mass ratio for Pageos that is most consistent with these data is

$$A/m = 132 \pm 4 \text{ cgs} \quad .$$

ACKNOWLEDGMENT

This work was supported in part by grant NGR 09-015-002 from the National Aeronautics and Space Administration.

REFERENCES

Aardoom, L., Girnius, A., and Veis, G., 1967. Determination of the absolute space directions between Baker-Nunn camera stations. In The Use of Artificial Satellites for Geodesy, vol. II, ed. by G. Veis, National Tech. Univ., Athens, pp. 315-344.

Aksnes, K., 1969. A second order solution for the motion of an artificial satellite based on an intermediate orbit. Ph.D. Thesis, Yale University.

Aksnes, K., 1975. Short-period and long-period perturbations of a spherical satellite due to direct solar radiation. Celest. Mech., in press.

Brachet, G., 1970, International Satellite Geodesy Experiment — ISAGEX. Centre National d'Etudes Spatiales. Report ISAGEX /7/CNES, November, 193 pp.

Brachet, G., 1973. International Satellite Geodesy Experiment — Report on data reduction and distribution. Centre National d'Etudes Spatiales, Report ISAGEX /17/CNES, July, 210 pp.

Brouwer, D., 1959. Solution of the problem of artificial satellite theory without drag. Astron. Journ., vol. 64, pp. 378-397.

Gaposchkin, E.M., editor, 1973. 1973 Smithsonian Standard Earth (III). Smithsonian Astrophys. Obs. Spec. Rep. No. 353, 388 pp.

Gaposchkin, E.M., 1974. Earth's gravity field to the eighteenth degree and geocentric coordinates for 104 stations from satellite and terrestrial data. Journ. Geophys. Res., vol. 79, pp. 5377-5411.

Gaposchkin, E.M., Latimer, J., and Mendes, G., 1974. Station coordinates in the Standard Earth III system derived using camera data from ISAGEX. Presented at INTERCOSMOS Meeting, Budapest, October.

Georgiev, N., and Sorokin, N.A., 1975. The preliminary determination of the coordinates of Baja and Sofia in the "Standard Earth" system. Presented at the XVIIIth COSPAR meeting, Varna, Bulgaria, June.

Karský, G., Kostelecký, J., Skoupý, V., and Synek, I., 1974. The determination of station 1147 coordinates. Presented at the XVIIth COSPAR Meeting, São Paulo, Brazil, June.

Kovalevsky, J., 1974. Results of the "ISAGEX" campaign. Presented at the XVIIth COSPAR Meeting, São Paulo, Brazil, June.

Kozai, Y., 1961. Effects of solar radiation pressure on the motion of an artificial satellite. Smithsonian Astrophys. Obs. Spec. Rep. No. 56, pp. 25-33.

Kozai, Y., 1962. Second-order solution of artificial satellite theory without air drag. Astron. Journ., vol. 67, pp. 446-461.

Kozai, Y., 1963. Effects of solar radiation pressure on the motion of an artificial satellite. Smithsonian Contr. Astrophys., vol 6, pp. 109-112.

Lautman, D.A., 1975a. Perturbations of a close-earth satellite due to sunlight diffusely reflected from the earth. Submitted to Celest. Mech.

Lautman, D.A., 1975b. Perturbations of a close-earth satellite due to sunlight diffusely reflected from the earth. II. Variable albedo. To be submitted to Celest. Mech.

Lerch, F.J., Wagner, C.A., Richardson, J.A., and Brownd, J.E., 1974. Goddard Earth Models (5 and 6). Goddard Space Flight Center Document X-921-74-145, December, 310 pp.

Lucas, J.R., and Chovitz, B.H., 1971. Tests on the Smith model for perturbations of balloon satellites. Presented at the XIVth COSPAR Meeting, Seattle, Washington, June.

Lundquist, C. A., and Veis, G., editors, 1966. Geodetic Parameters for a 1966 Smithsonian Institution Standard Earth. Smithsonian Astrophys. Obs. Spec. Rep. No. 200, 3 vols., 686 pp.

Prior, E.J., 1970. Earth albedo effects on the orbital variations of ECHO I and PAGEOS I. In Dynamics of Satellites 1969, ed. by B. Morando, Springer-Verlag, Berlin, pp. 303-312.

Slowey, J.W., 1974. Radiation-pressure and air-drag effects on the orbit of the balloon satellite 1963 30D. Smithsonian Astrophys. Obs. Spec. Rep. No. 356, 85 pp.

Smith, D.E., and Kissell, K.E., 1971. Anomalous accelerations of the PAGEOS spacecraft. Goddard Space Flight Center Document X-553-71-338, August, 6 pp.

Smith, D.E., Lerch, F.J., and Wagner, C.A., 1973. A gravitational field model for the earth. In Space Research XIII, ed. by M.J. Rycroft and S.K. Runcorn, Akademie-Verlag, Berlin, pp.11-20.

Table 1. Basic constants.

GM	$= 3.986013 \times 10^{20}$ cm^3 sec^{-2}
c	$= 2.997925 \times 10^{10}$ cm sec^{-1} = velocity of light
k_2	$= 0.25$, $c_2 = 10°$ = tidal parameters
a_e	$= 6.378140 \times 10^8$ cm
α	$= 0.219 + 0.410 \sin^2 \phi$ = earth's albedo
E_{IR}	$= 0.380 - 0.117 \sin^2 \phi$ cal cm^{-2} min^{-1}=earth's infrared emissivity

Table 2. Total number of camera observations available from AFU-75 during ISAGEX.

Station		Satellite				Totals
		6102801	6508901	6605601	6800201	
Uzhgorod	1055	185	88	1729	27	2029
Riga	1084	20	70	353	39	482
Cairo	1901	520	52	1005	129	1706
Potsdam	1181	55	24	---	65	144
Delft	8034	---	---	---	139	139
Zvenigorod	1072	118	45	397	15	575
Ondrejov	1147	6	215	---	78	299
Sofia	1101	---	---	434	---	434
Baja	1113	16	---	133	---	149
Bucharest	1131	9	---	327	---	336
Sakhalin	1065	174	---	---	---	174
Ulan Bator	1660	212	30	22	26	290
Kerguelen	1108	101	---	4	---	105
						6862

Table 3. Total number of AFU-75 camera observations used in the preliminary analysis (Gaposchkin et al., 1974).

Station		Satellite				Totals
		6102801	6508901	6605601	6800201	
Uzhgorod	1055	75	36	559	1	671
Riga	1084	20	38	45	16	119
Cairo	1901	360	17	68	24	469
Potsdam	1181	9	58	---	18	85
Delft	8034	---	---	---	47	47
						1391

Table 4. Total number of camera observations from ISAGEX used in the final analysis.

	Initial time	41011	41136	40998	41018	41036	41133	41152	40987	41010	41018	41057	41064	41100	40992	41036	41042	41054	41176	Totals
	Satellite	6102801	6102801	6508901	6508901	6508901	6508901	6508901	6605601	6605601	6605601	6605601	6605601	6605601	6800201	6800201	6800201	6800201	6800201	
Uzhgorod	1055	105	54	17			64		152	340	223	426	234					7		1622
Riga	1084	20		7	31				218									7		283
Cairo	1901	112	343				15	33	277		57	176	230	54			1	8	39	1345
Potsdam	1181		13	9	12		3								6					63
Delft	8034															17		10	20	47
Zvenigorod	1072	100		41	4							65	24	155	13		26			428
Ondrejov	1147		5	11	66		28										4	12	23	149
Baja	1113		6									107								113
Bucharest	1131		4							52		225								281
Sofia	1101																			
Sakhalin	1065	151																		151
Ulan Bator	1660	166		29														24		219
Kerguelen	1108	70																		70
																				4771

Table 5. Potential simultaneous data.

Type of observation	Satellite positions	Synthetic observations	Actual observations
Flash (Geos 2)	205	454	454
Passive (all satellites)	112	229	1892
Total	317	683	2346

Table 6. Final simultaneous data.

Type of observation	Satellite positions	Synthetic observations	Actual observations
Flash (Geos 2)	114	259	259
Passive (all satellites)	68	137	1164
Total	182	396	1423

Table 7. ISAGEX geometrical adjustment.

Fixed stations		Determined stations	
8009	Haute Provence	1055	Uzhgorod
8019	Nice	1072	Zvenigorod
9004	San Fernando	1084	Riga
9028	Addis Ababa	1147	Ondrejov
9030	Dionysos	1901	Cairo
9091	Athens	8034	Delft
		1181	Potsdam
		8010	Zimmerwald
		8011	Malvern

Table 8. Adjustable synchronous planes between stations.

Station pair	No. of planes	Station pair	No. of planes
1181–8011	5	8034–8011	6
1181–9004	10	8034–9030	12
1901–9004	7	1072–8019	4
1055–9004	1	8019–8034	6
1901–9028	6	8010–8034	13
1055–1084	16	1147–8009	8
1055–1901	17	1147–8010	11
1901–9030	8	1084–8009	6
1055–9030	3	8034–8009	11
1084–1147	1	8034–9004	29
1072–9030	1	1147–8034	4
1055–1147	8	1147–9004	5
1084–1901	9	1055–8034	5
1072–1901	1	1084–8034	4
1055–1072	1	1147–9030	13
Total		30 pairs	231

Table 9. Selected arcs for this analysis.

Satellite	Initial time (MJD)	Final time (MJD)
6102801	41011	41044
6102801	41136	41184
6508901	40998	41014
6508901	41018	41026
6508901	41036	41044
6508901	41133	41146
6508901	41152	41163
6605601	40987	40994
6605601	41010	41015
6605601	41018	41023
6605601	41057	41063
6605601	41064	41071
6605601	41100	41107
6800201	40992	41009
6800201	41036	41042
6800201	41042	41048
6800201	41054	41062
6800201	41176	41189

Table 10. Adopted combination solution for station coordinates.

Station	X (Mm)	Y (Mm)	Z (Mm)	Root mean variance (m)
1055	3.9074193	1.6024293	4.7638880	5.1
1072	2.8861977	2.1559926	5.2458182	10.4
1084	3.1838800	1.4214690	5.3227997	4.5
1147	3.9784508	1.0510261	4.8575649	4.7
1181	3.8005960	.8819889	5.0288652	9.3
1901	4.7283132	2.8796241	3.1568625	4.6
8034	3.9196518	.2988409	5.0058938	4.4
1660	-1.2574253	4.0993462	4.7080078	9.5
1108	1.4078163	3.9178375	-4.8160060	44.5
8010	4.3313028	.5675259	4.6331040	3.2
8011	3.9201612	-.1347344	5.0127256	4.0

Table 11. Comparison of ellipsoid height for stations determined.

Station		Global system				EUR 50 system			
		h_{msl}	h_{geoid}	h_{ellip}	$h_{ellip} - (h_{geoid} + h_{msl})$	h_{geoid}	h_{ellip}	$h_{ellip} - (h_{geoid} + h_{msl})$
1055	Uzhgorod	189	31	204.63	-15	- 1.5	185.01	- 2.49
1072	Zvenigorod	173	12	144.09	-41	-10.0	138.65	-24.35
1084	Riga	8	16	10.82	-13	- 5.6	2.08	- 0.32
1181	Potsdam	109.2	35	132.11	-12	0.0	111.87	2.57
8034	Delft	6.00	40	12.87	-33	- 3.7	-18.85	-21.15
8011	Malvern	113.2	47	149.58	-11	- 4.6	109.39	0.79
8010	Zimmerwald	903.44	44	932.76	-15	- 3.1	895.29	- 5.05
1147	Ondrejov	506	38	549.13	- 5	4.5	524.87	14.37
1901	Cairo	120	2	114.07	- 8			
1660	Ulan Bator	1607	-24	1549.84	-33			
1108	Kerguelen	50	28	74.90	- 3			
1065	Sakhalin	38	30					

FIGURE CAPTIONS

Figure 1. Locations of ISAGEX laser and camera stations.

Figure 2. The local network in Europe.

Figure 3. Mean elements and perturbations for Pageos.

Figure 4. The effects of the 10.7-cm solar flux on the orbital acceleration of Pageos. a) $\dot{n}$, the orbital acceleration of Pageos; b) $F_{10.7}$, the 10.7-cm solar flux.

Figure 5. General processing scheme.

Figure 6. Additional geometrical data.

Figure 7. Comparisons of interstation directions from the combination, dynamical, and geometrical solutions. ψ is in the direction of increasing declination, and μ is in the direction of increasing right ascension.

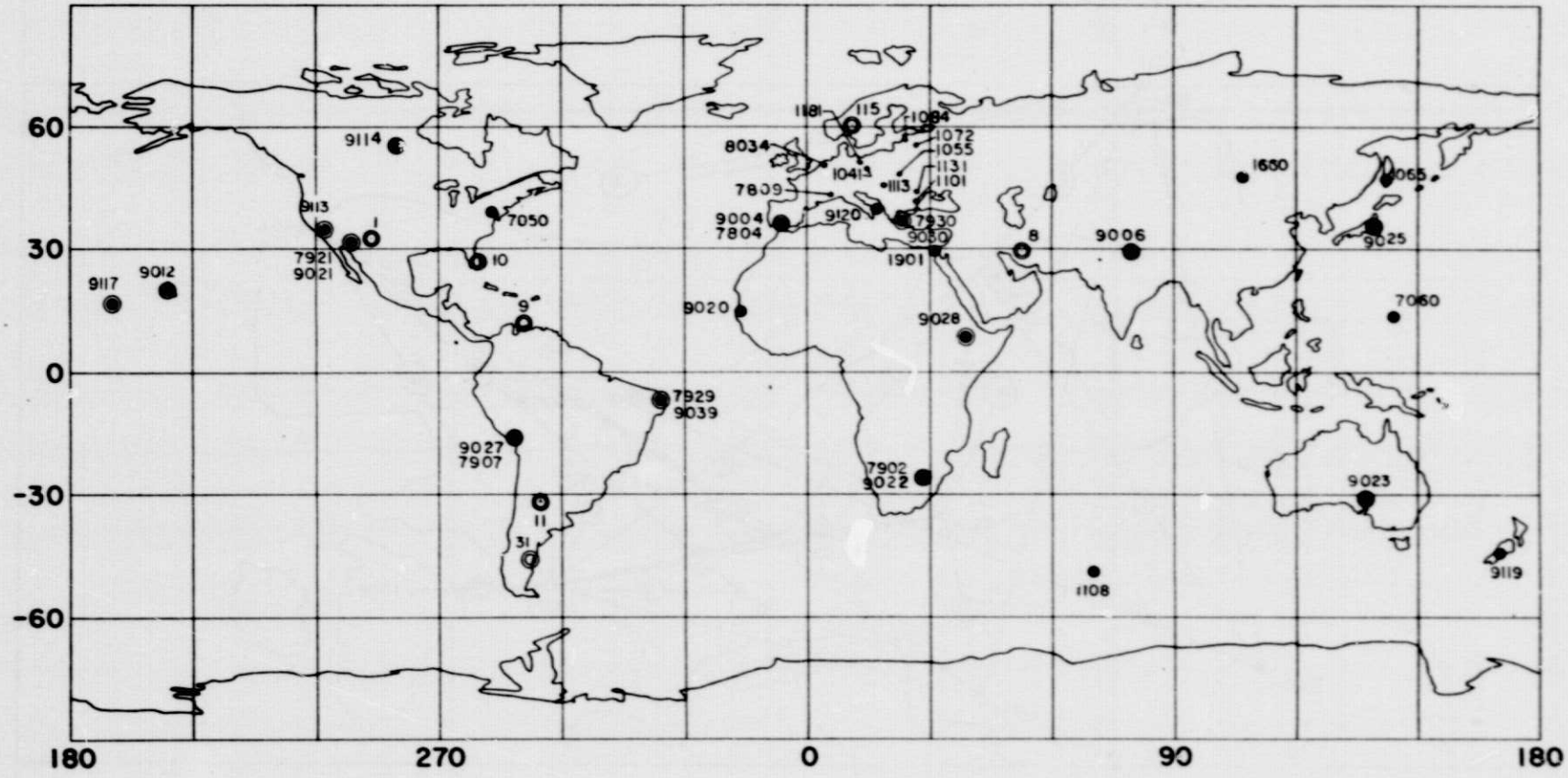

Figure 1. Locations of ISAGEX laser and camera stations.

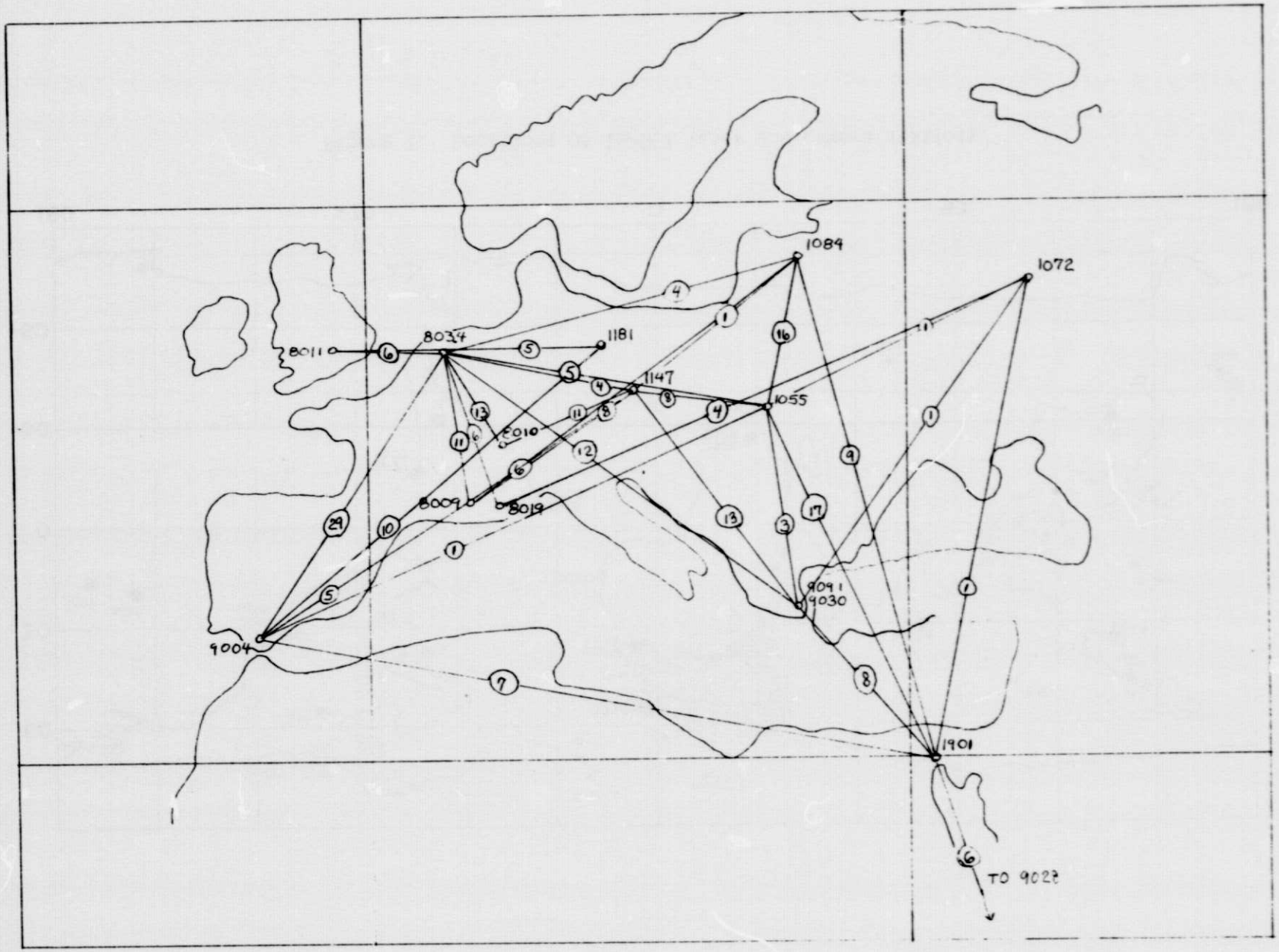

Figure 2. The local network in Europe.

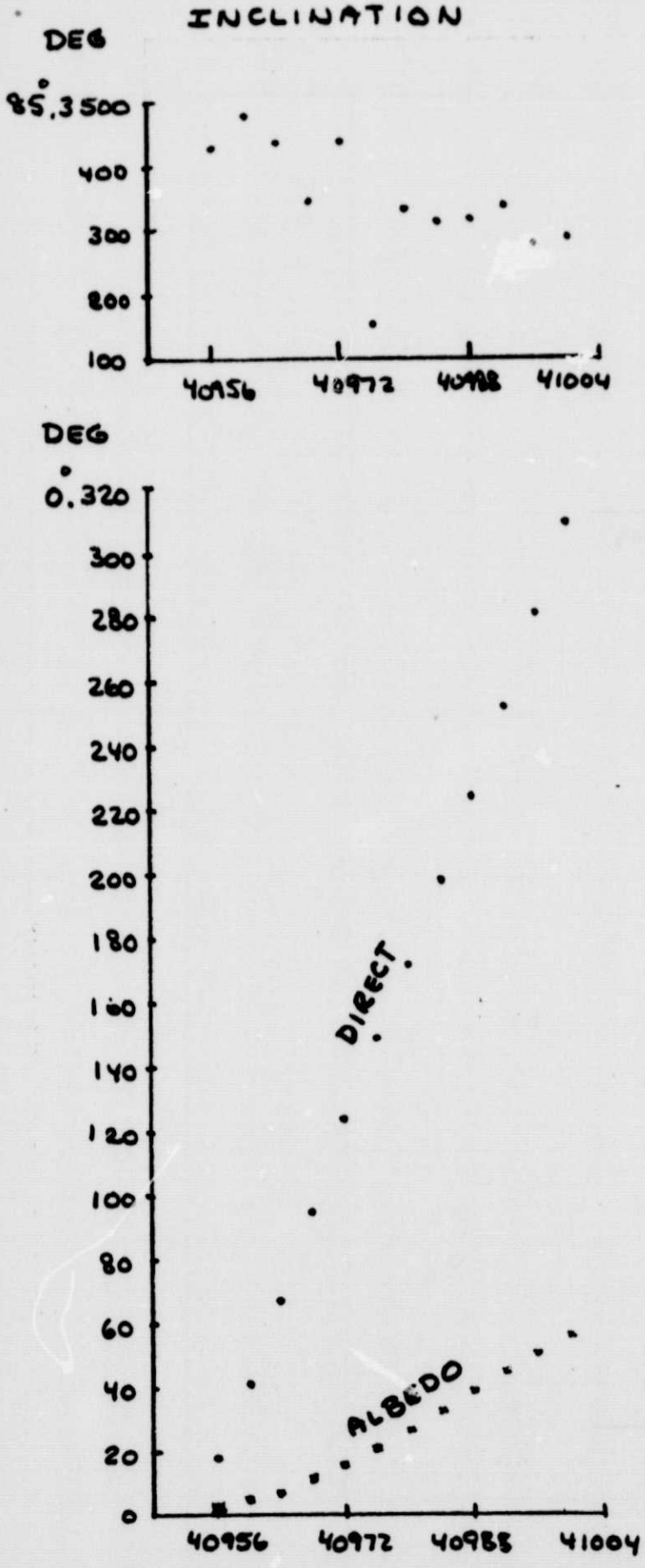

Figure 3. Mean elements and perturbations for Pageos.

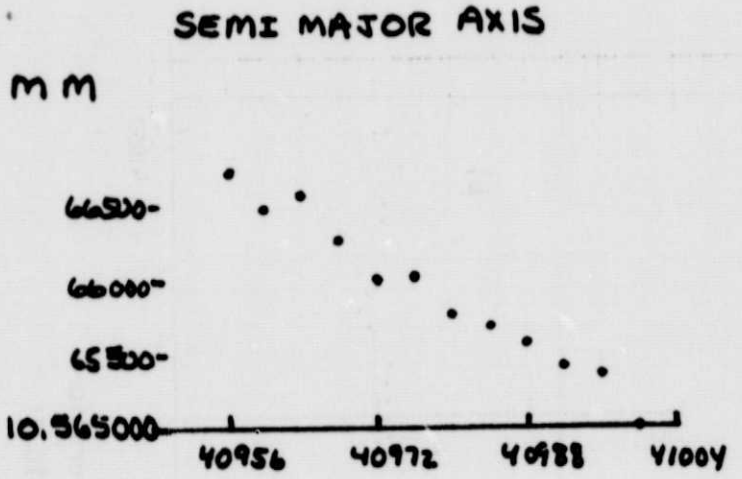

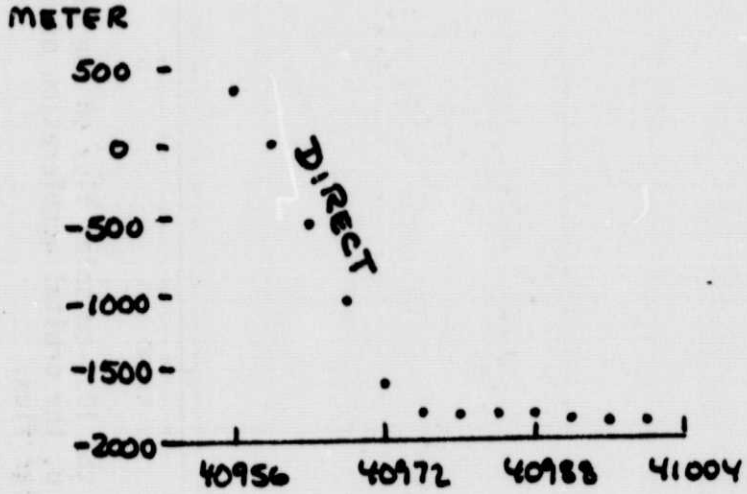

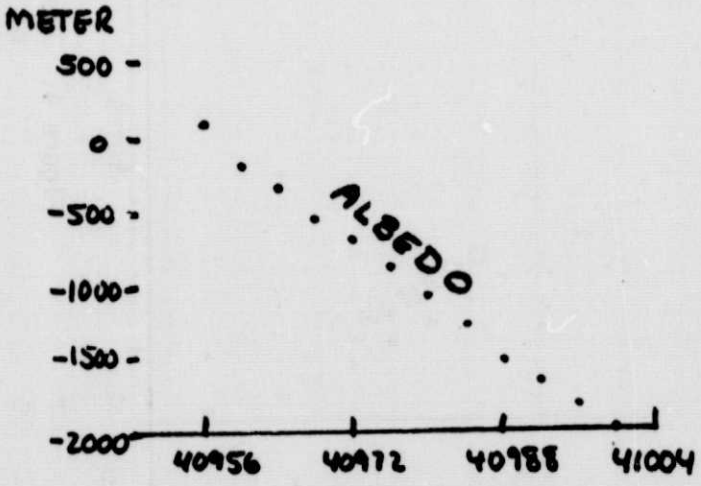

Figure 3. (Cont.)

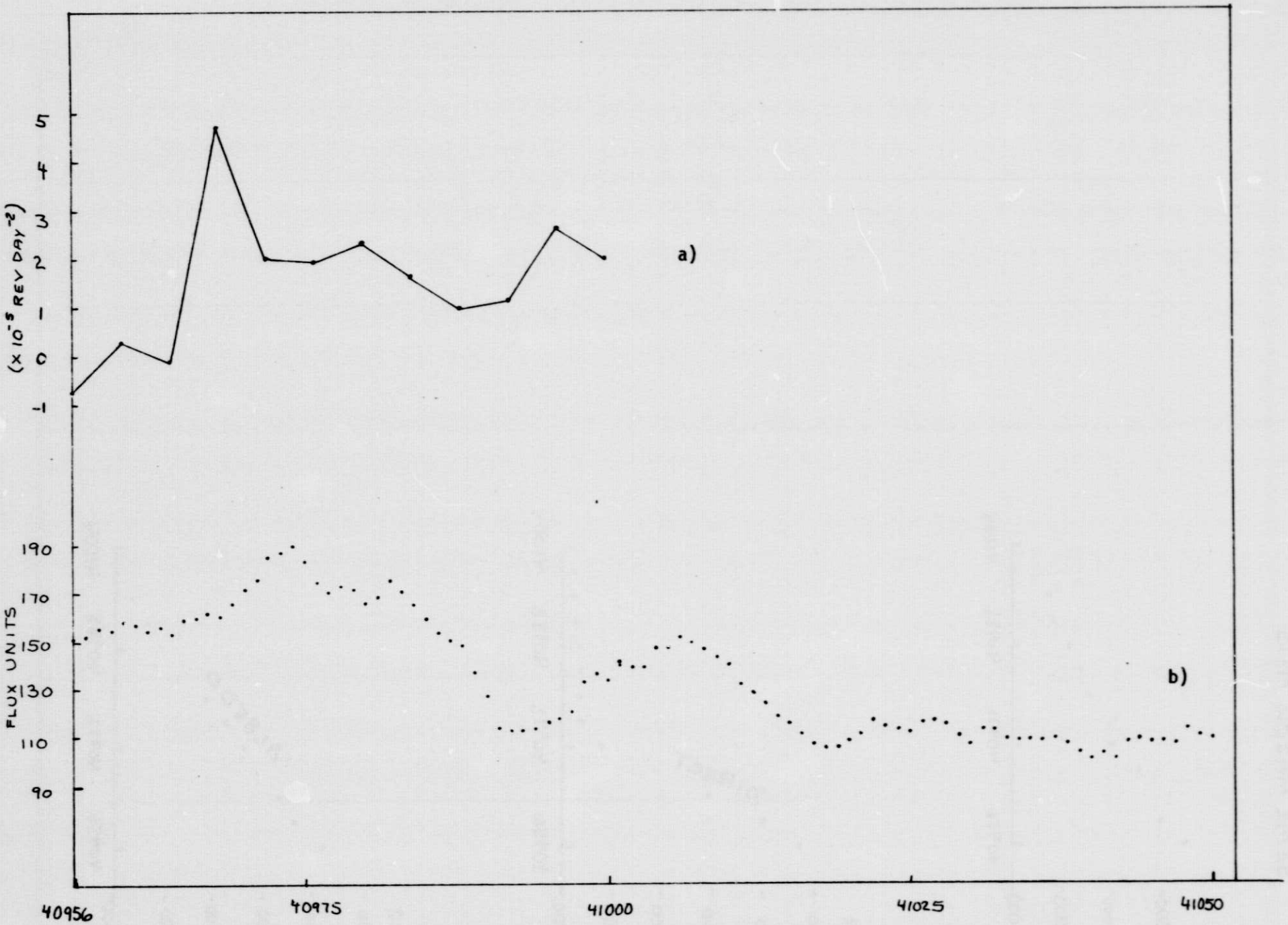

Figure 4. The effects of the 10.7-cm solar flux on the orbital acceleration of Pageos. a) $\dot{n}$, the orbital acceleration of Pageos; b) $F_{10.7}$, the 10.7-cm solar flux.

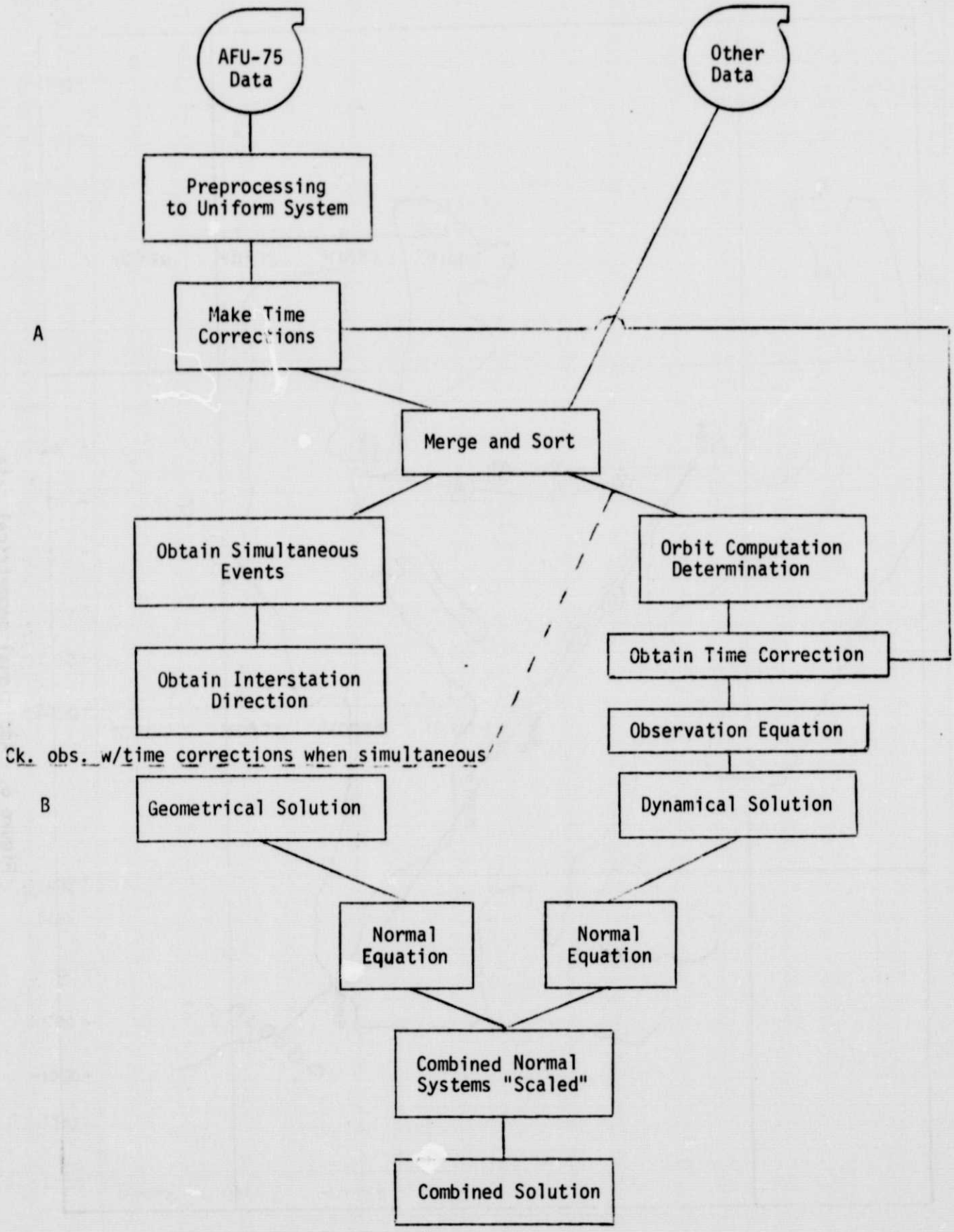

Figure 5. General processing scheme.

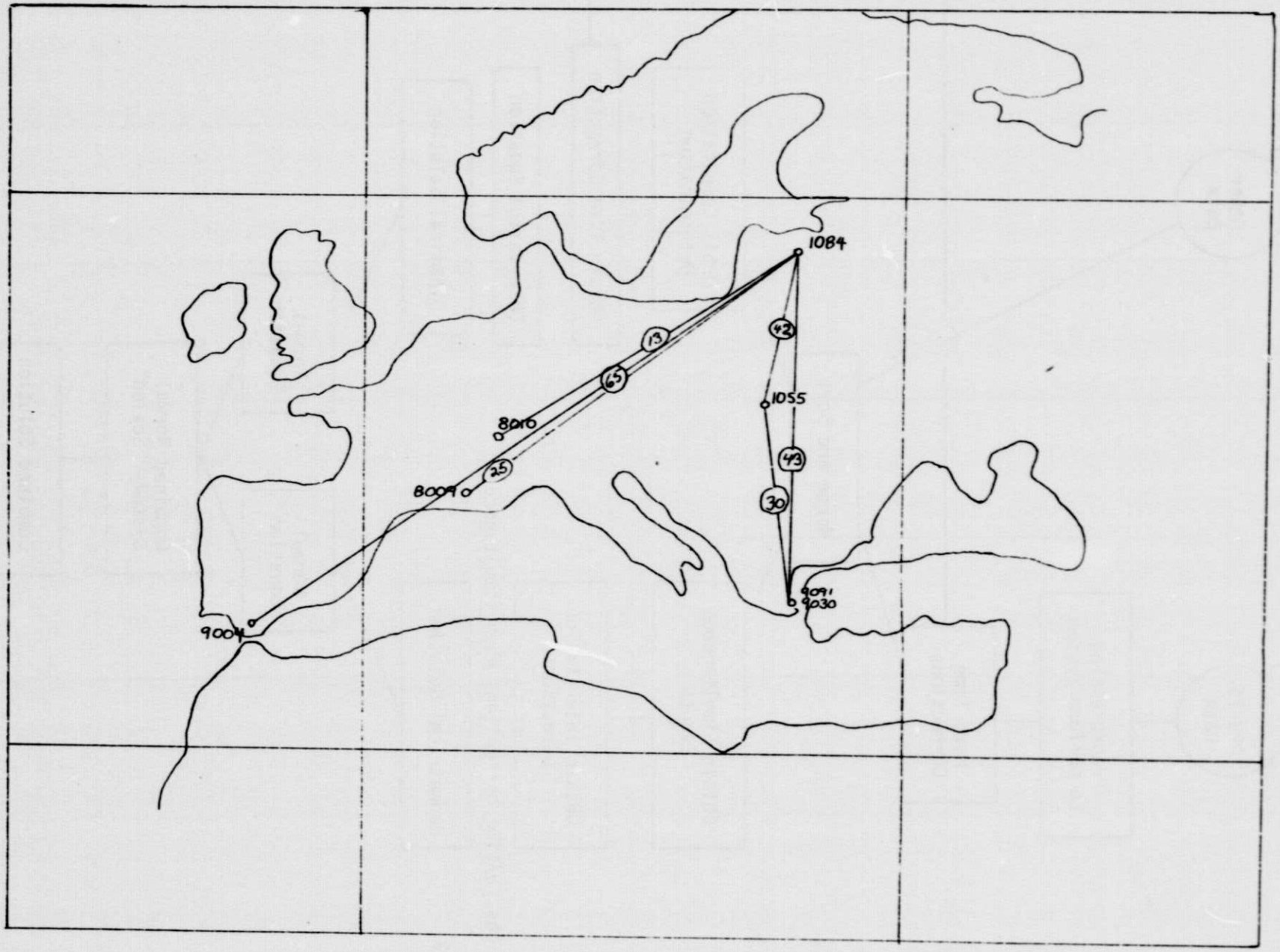

Figure 6. Additional geometrical data.

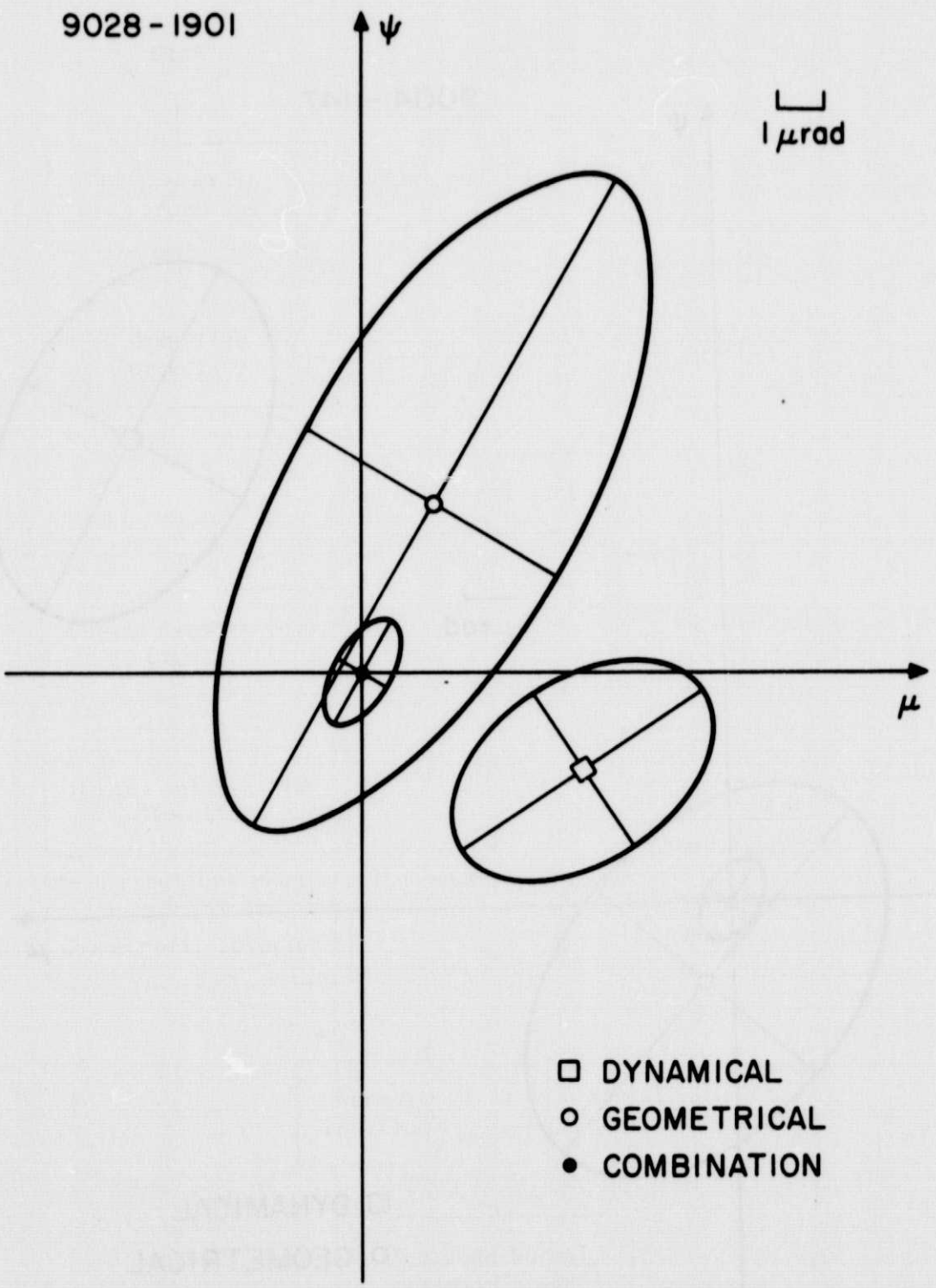

Figure 7. Comparisons of interstation directions from the combination, dynamical, and geometrical solutions. ψ is in the direction of increasing declination, and μ is in the direction of increasing right ascension.

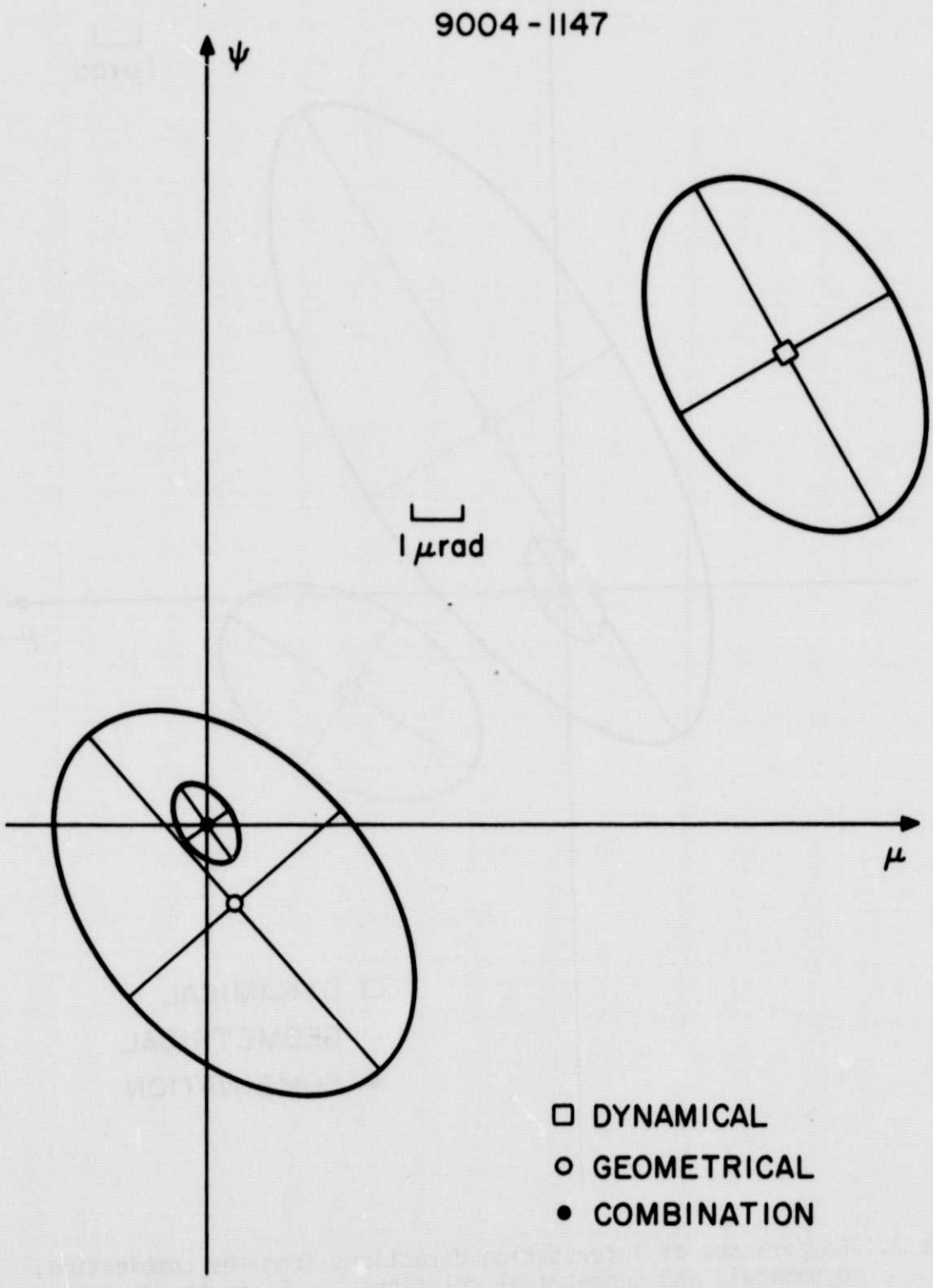

Figure 7. Comparisons of interstation directions from the combination, dynamical, and geometrical solutions. ψ is in the direction of increasing declination, and μ is in the direction of increasing right ascension.

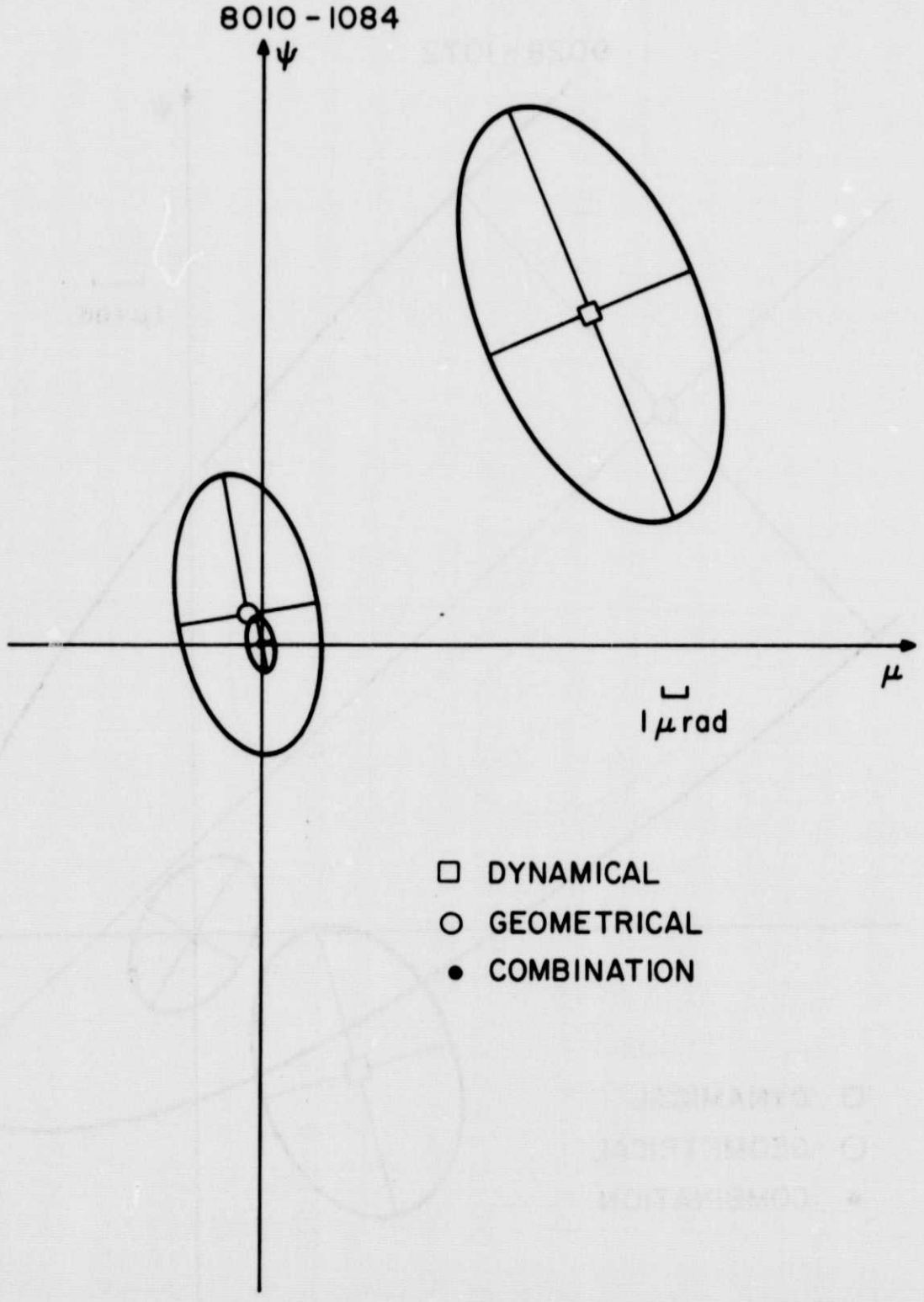

Figure 7. Comparisons of interstation directions from the combination, dynamical, and geometrical solutions. ψ is in the direction of increasing declination, and μ is in the direction of increasing right ascension.

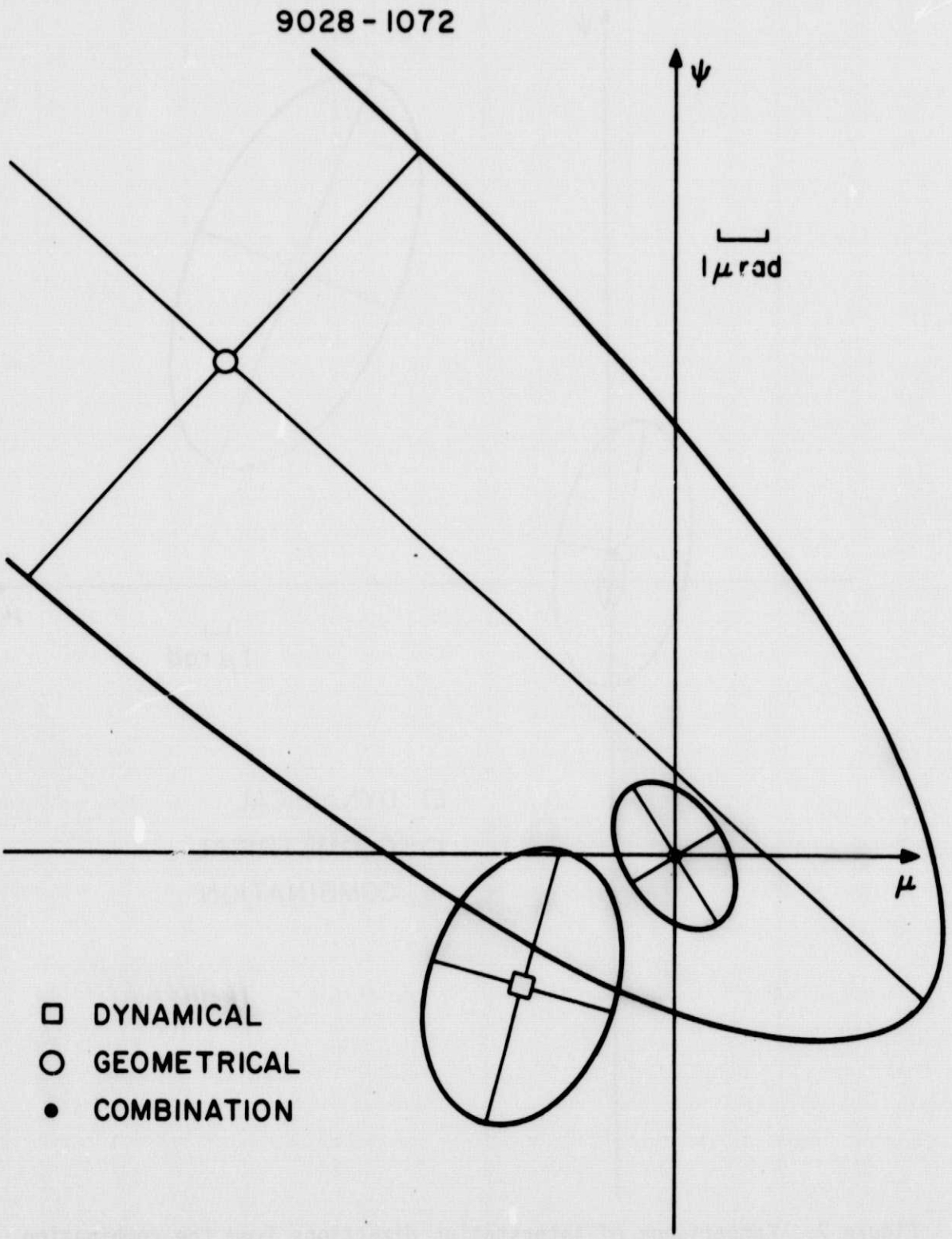

Figure 7. Comparisons of interstation directions from the combination, dynamical, and geometrical solutions. ψ is in the direction of increasing declination, and μ is in the direction of increasing right ascension.